JOURNAL OF GEOPHYSICAL RESEARCH, VOL. 113, D24S90, doi:10.1029/2008JD010276, 2008

Aerosol relationships to warm season clouds and rainfall at monthly scales over east China: Urban land versus ocean

Menglin Jin[1] and J. Marshall Shepherd[2]

Received 15 April 2008; revised 10 August 2008; accepted 17 September 2008; published 31 December 2008.

[1] This paper provides a prototype study on combining the advanced satellite observations of rainfall, clouds, and aerosols to examine their interrelationships. Monthly satellite observations from the Tropical Rainfall Measuring Mission (TRMM) and Moderate Resolution Imaging Spectroradiometer (MODIS) for July (2000–2005) were analyzed to assess how urban aerosols affect cloud droplet size and cumulative rainfall over the eastern China mainland and the China Sea, respectively. It seems that aerosol effects may be more evident on clouds than on convective rainfall: high correlation coefficients between aerosol optical thickness (AOT) and water cloud droplet size are observed, while only a weak aerosol-rainfall relationship is detectable during light rainfall cases (i.e., rainfall rate < 2.5 mm/d) and that is most likely for warm rain clouds only. In addition, aerosols affect clouds more significantly over ocean than over land. Over the ocean, at the monthly scale, the aerosol-cloud relationship is evident: the cloud effective radius decreases as aerosol optical thickness (AOT) increases. However, over land, cloud effective radius does not show an apparent relationship with aerosol processes, which indicates that aerosols are not the only physical process affecting clouds. Dynamic processes related to factors like urban land cover may play at least an equally critical role in cloud formation.

Citation: Jin, M., and J. M. Shepherd (2008), Aerosol relationships to warm season clouds and rainfall at monthly scales over east China: Urban land versus ocean, *J. Geophys. Res.*, *113*, D24S90, doi:10.1029/2008JD010276.

1. Introduction

[2] Urban regions have unique aerosol, cloud, and rainfall properties [*Changnon et al.*, 1976; *Post and Buseck*, 1984; *Joseph et al.*, 1991; *Carrico et al.*, 2003, *Alpert et al.*, 2005, *Jin et al.*, 2005a]. One of the world's most dense aerosol regions is east Asia [*Li et al.*, 2007; *Duncan et al.*, 2003]. Urban regions over east China contain large volumes of aerosols, owing to both human activities (construction, traffic, etc.) and remote biomass burning or dust storms transported to the urban regions [*Jin and Shepherd*, 2005, *Zhao and Li*, 2007]. As a result of atmospheric transport, the China Sea also has relatively heavier aerosol concentrations than other open oceans throughout the year (see Figure 1).

[3] While the climate change discussion has focused on greenhouse gas forcing and its effects on the water cycle, the IPCC [*Trenberth et al.*, 2007] noted a growing interest in understanding what role urban land cover/land use (LCLU) and pollution (e.g., aerosols) have on hydroclimates. Urban pollution has been expected to affect precipitation processes. Assessing the effects of aerosols on clouds and rainfall is critical but challenging [*Rosenfeld et al.*, 2007; *Lensky and Drori*, 2007; *Vallina et al.*, 2006; *Li and Yuan*, 2006; *Bell et al.*, 2008] owing to the complexity of direct and indirect effects of aerosol processes. On one hand, anthropogenic aerosols increase cloud condensation nuclei (CCN) in the atmosphere. In situations where only limited water vapor is available, more CCN competing for water vapor to form cloud droplets would reduce the effective radius of cloud droplets. This is the so-called first aerosol "indirect effect" [*Twomey et al.*, 1984]. Smaller cloud droplets would suppress the development of rainfall [*Remer and Kaufman*, 1998; *Rosenfeld*, 2000]. Nevertheless, a recent study by *Lau et al.* [2006], via a climate model, showed that increased absorbing aerosols over the Indo-Gangetic Plain during the premonsoon season were partly responsible for the enhancement of the rainy monsoon season in northern India in May. Their model study suggests that this process leads to increased rainfall over the Indian subcontinent as well as decreased rainfall over East Asia in June–July. *Jacobson and Kaufman* [2006], also via model simulations, suggested another mechanism whereby aerosols suspended in the atmosphere reduce surface wind and reduce the recirculation of water and energy in a rainfall system. In summary, aerosols affect rainfall by changing radiation exchanges in the atmosphere and at the surface, namely "the direct effect" [*Kaufman et al.*, 2002; *Ramanathan et al.*, 2001; *Lau and Kim*, 2006], by its interaction with clouds ("the

[1]Department of Meteorology, San José State University, San José, California, USA.

[2]Atmospheric Sciences Program, Department of Geography, University of Georgia, Athens, Georgia, USA.

0148-0227/08/2008JD010276$09.00

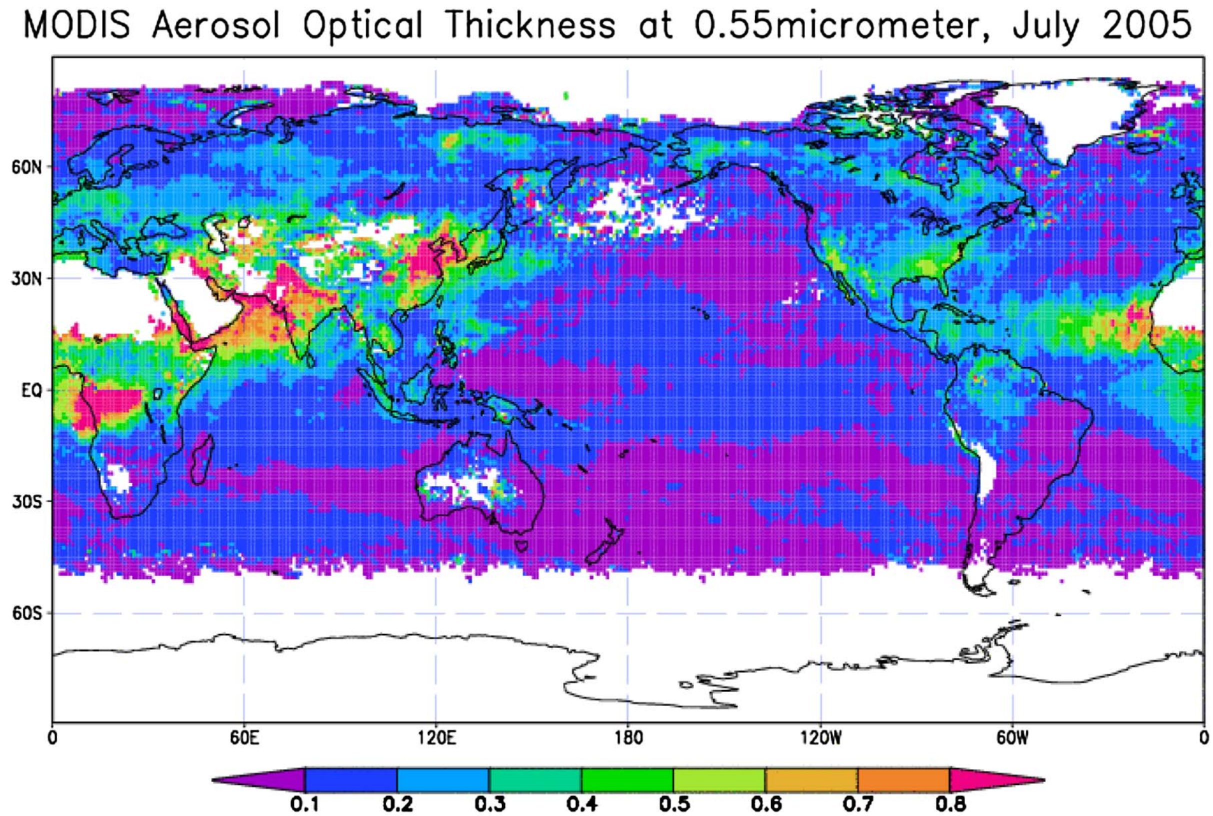

Figure 1. Global distribution of aerosol optical thickness at 0.55 μm observed from NASA Terra MODIS at 1030 local time for July 2005. MODIS aerosol observations have 10 km $\times$ 10 km resolution and are aggregated to 1° $\times$ 1°. White areas constitute no retrievals owing to snow or bright desert surfaces or lack of sunlight.

indirect effect'') [*Kaufman et al.*, 2002], and by other geophysical-chemical-dynamical processes, such as changing wind speed or chemical interactions [*Jacobson and Kaufman*, 2006].

[4] The complexity of aerosol effects on clouds and rainfall in urban regions is due to the fact that, in addition to aerosol-related processes, local dynamics and thermodynamics related to the urban environment (for example, urban heat island-induced circulations and mechanical turbulence-induced convergence) also affect physical-dynamical processes related to precipitation [*Shepherd*, 2005]. Most historical and current literature indicates that rainfall increases over urban and downwind regions [*Changnon et al.*, 1976; *Shepherd et al.*, 2002; *Burian and Shepherd*, 2005; *Mote et al.*, 2007]. In this study, we aim to examine the aerosol effect on clouds and rainfall, and further discuss the relative contribution of this effect and dynamic mechanisms to clouds and rainfall.

[5] Current understanding of aerosol effects on clouds and rainfall is far from complete. There are essentially three types of research approaches: one uses climate models to examine aerosol effect on clouds/rainfall [e.g., *Jacobson and Kaufman*, 2006; *Lau et al.*, 2006]. However, the model is largely limited by questionable aerosol/cloud/rainfall parameterization, and thus may lead to unrealistic results. The second approach is based on a relatively limited data from field experiments over a small region [e.g., *Rosenfeld*, 2000]. This approach is typically unable to resolve the spatial, temporal, and feedback complexities that characterize the aerosol-cloud-rainfall relationships in the real world. The third approach is to analyze rainfall variability and couple it with aerosol changes, and assume some degree of correlation or causality [e.g., *Berg et al.*, 2006; *Lau and Kim*, 2006; *Zhao et al.*, 2006]. Although these three approaches shed unique light on aerosol effects, they all have severe limitations. More observational research incorporating temporally and spatially consistent aerosol, cloud, and rainfall data is needed to acquire further understanding of aerosol effects.

[6] One of the biggest challenges in observational aerosol effect studies is obtaining the temporally and spatially consistent observations for aerosols, clouds, and rainfall. In general, remote sensing techniques cannot measure aerosols when clouds and rainfall are present. For example, in this work, 5 years of National Aeronautics and Space Administration (NASA) Tropical Rainfall Measuring Mission (TRMM) measurements and Moderate Resolution Imaging Spectroradiometer (MODIS) measurements for July (2000–2004) were used to examine summer rainfall events. Aerosol-cloud-rainfall variability studies require accurate measurements of the three variables (e.g., clouds, aerosols, and rainfall). However, current cloud and aerosol measurements

from MODIS are not able to examine instantaneous aerosol effects because the MODIS instrument cannot measure aerosols under cloudy or rainy conditions. The most practical approach, as we suggest here, may be to examine climatological relationships at a monthly scale to establish whether, in a climatological sense, aerosols demonstrate strong correlations to clouds and rainfall. Uncertainty exists because of the inconsistency of data, but the exercise still provides a credible assessment of first-order relationships among monthly aerosols, clouds, and rainfall. In addition, July is our focus because (1) it represents the period of the monsoon season of east China, in which the majority of rainfall is from convection and (2) aerosol optical thickness (AOT) there is generally high during summer. Aerosol effects, if any, would presumably be easier to detect during this time period. In their seasonal analysis of Beijing's air quality, *Zheng et al.* [2005] noted that the majority of the particulate matter in Beijing during July is anthropogenic. Dust was a secondary contributor but biomass burning aerosols were at a minimum.

[7] Our new findings are that, at monthly scale, a significant aerosol effect is detectable in cloud microphysical fields (i.e., cloud effective radius), and a weaker aerosol effect is detectable in light, warm, oceanic rainfall events. Comparisons between ocean and land reveal that aerosol effects are more evident over light, oceanic rainfall cases than over land. In general, aerosol effects on cloud properties seem to be more significant than on rainfall variability. The broader impact is that, through the research approach presented here, we can evaluate whether urban aerosols indirectly modify both land-based as well as oceanic surface rainfall through aerosol-cloud interactions.

[8] Temporal scale is a critical issue in aerosol-cloud-rainfall analyses. We analyze monthly scale aerosols and rainfall to see if there is clear signal between them. Because the aerosol optical thickness (AOT) data is retrieved for cloud-free pixels, it is impossible to study instantaneous relationships between aerosol and rainfall for a given pixel at a particular time. Nevertheless, a large body of research has shown that averaged values can present the signal of physical processes in a climatological sense. One example of this is boundary layer statistics: it is difficult to ascertain how one particular air molecule moves, but the average of its movement, air temperature, is quite useful. A similar philosophy is adopted in our examination of aerosol-cloud-rainfall relationships at monthly scale.

[9] The next section (section 2) describes the rainfall efficiency, a new variable derived from active and passive microwave retrievals to better represent aerosol effects on rainfall. Section 3 describes the data sets used. Section 4 discusses the results, followed by a section of final discussion and remarks (section 5).

2. Method and Approach

[10] In order to more efficiently demonstrate aerosol effects on rainfall, we define a new variable: rainfall efficiency (G),

$$G = PR_{rate}/CLW, \quad (1)$$

in which PR_{rate} is precipitation rate measured by TRMM's Precipitation Radar (PR), in units of mm/d. CLW is cloud liquid water (mm), which is retrieved from the Special Sensor Microwave/Imager (SSM/I) data (http://www.ssmi.com/ssmi/ssmi_description.html). As a result, G has units of 1/d. It should be noted that the absolute value of Γ may not be the accurate "efficiency," but to a certain degree it reflects how efficient the rainfall process is.

[11] This definition of G follows *Berg et al.* [2006] in which G was proven to be an insightful estimation of rainfall efficiency. The underlying physical basis for such a new variable is that the TRMM radar measurements are sensitive to the size of raindrops while the SSMI microwave retrieval is sensitive to cloud liquid water. Therefore, PR_{rate} derived from the TRMM radar accounts for the change of cloud droplet size induced by aerosols, while the microwave retrieval of CLW does not account for such change. As a result, the ratio of PR_{rate} and CLW removes part of the information that is not sensitive to aerosols, and thus Γ is expected to be more sensitive to aerosol effects on rainfall, if any (R. F. Adler, personal communication, 2006).

[12] The TRMM PR is a unique instrument that "provides three-dimensional profiles of storm structure as well as intensity and vertical and horizontal distribution of precipitation and precipitation type" [*National Research Council*, 2006]. This work offers a prototype of how to wisely use TRMM PR data in aerosol-rainfall studies.

[13] Owing to the different mechanisms for rainfall, aerosol effects on clouds and rainfall are traditionally considered to be different for convective rainfall and stratiform rainfall, and for the rainfall amount (light or heavy). We divide the rainfall events into five categories from light to heavy: < 0.5 mm/d, 0.5–2.5 mm/d, 2.5–5 mm/d, 5–10 mm/d, and > 10 mm/d. In this way, we are able to examine how aerosols affect rainfall in various categories.

3. Data

[14] Monthly rainfall measurements from TRMM for July (2000–2004), in particular, the rainfall rate from the PR (downloadable from NASA DAAC http://disc2.nascom.nasa.gov/Giovanni/tovas/) and cloud liquid water from SSM/I version 6 (http://www.ssmi.com/ssmi/ssmi_description.html) are used. TRMM is a joint U.S. and Japanese mission that was launched in 1997 to advance the understanding of the global energy and water cycle by providing distributions of rainfall and latent heating over the global tropics [*Simpson et al.*, 1988; *Adler et al.*, 2000]. The TRMM PR is the world's first spaceborne precipitation radar and operates at a frequency of 13.8 GHz. SSM/I flies on the polar-orbiting Defense Meteorological Satellite Program (DMSP) satellites. The SSM/I is a microwave radiometer with dual-polarized channels ranging from 10 to 87 GHz (also one vertically polarized channel at 22 GHz). These frequencies are typically used to retrieve liquid water path of precipitating and nonprecipitation clouds, although each algorithm varies [*Alishouse et al.*, 1990; *Jung et al.*, 1998]. Specifically, we use the 3A25 monthly, $0.5° \times 0.5°$ rain rate product retrieved from the TRMM PR. This gridded version of the standard algorithm corrects for attenuation following techniques described by *Iguchi et al.* [2000]. The PR data is

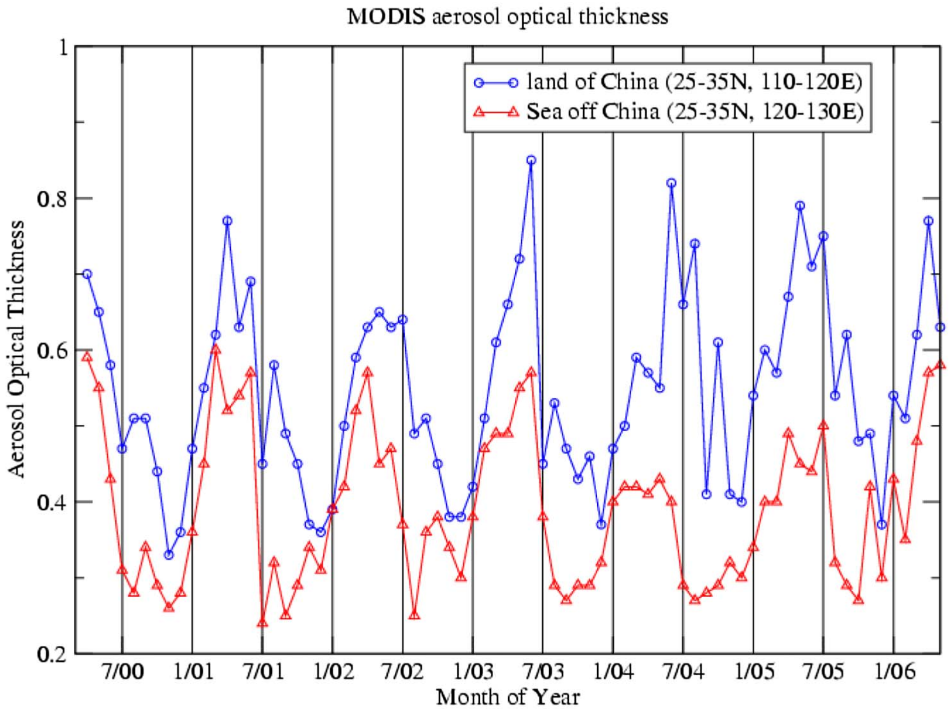

Figure 2. Interannual variations of urban aerosols over land (25°N–35°N, 110°E–120°E) and the sea off China (25°N–35°N, 120°E–130°E).

combined with cloud liquid water data retrieved from the unified ocean parameter retrieval algorithm of *Wentz and Spencer* [1998]. The algorithm, using fundamental radiative transfer principles, retrieves near surface wind speed, columnar water vapor, columnar cloud liquid water content, rain rate, and effective radiative temperature of upwelling radiation. This algorithm also minimizes cross contamination among product retrievals. The cloud liquid water data was accessed from the RSS website (http://www.ssmi.com/ssmi/ssmi_browse.html).

[15] Corresponding monthly MODIS aerosol optical thicknesses at 0.55 μm are analyzed. Recently available MODIS observations have overcome the difficulties of aerosol retrieval over land and now enable continental and oceanic aerosol measurements. Advantages of MODIS data include: (1) high spatial resolution whereby aerosol optical properties are derived for nonsnow and nondesert surfaces at 1 km $\times$ 1 km resolution and aggregated to 10 km $\times$ 10 km and 1° $\times$ 1° on a daily, 8-day, and monthly basis [*King et al.*, 2003]; (2) global observations twice per day at 1030 and 1330 local time (LT) from March 2000 (Terra) and 1330 and 0130 LT from July 2002 (Aqua) to present; and (3) global coverage. Cloud optical properties are available at a spatial resolution of 1 km $\times$ 1 km, and aggregated globally to 1° $\times$ 1°. These simultaneous observations make it possible to study urban regions over the globe.

[16] Five years (April 2000 to April 2005) of cloud property data, including effective radius for liquid water and ice clouds measured by MODIS [*King et al.*, 2003; *Platnick et al.*, 2003] were used in this study. MODIS uses infrared bands to determine cloud physical properties related to cloud top pressure and temperature, and visible and near-infrared bands to determine cloud optical and microphysical properties. *Nakajima and King* [1990] showed that the reflection function of clouds at a nonabsorbing band in the visible wavelength region (e.g., 0.66 μm) is primarily a function of cloud optical thickness, whereas the reflection function at a liquid water (or ice) absorbing channel in the near-infrared (i.e., 1.6 or 2.1 μm) is a function of cloud particle size. This algorithm includes extensions to distinguish between liquid water and ice clouds and to consider reflection by various underlying surfaces, including snow and sea ice [*King et al.*, 2004]. It also has been incorporated into the operational MODIS retrieval algorithm. MODIS provides cloud effective radius (r_e) in two thermodynamic phases, viz., liquid water (r_{ew}) and ice (r_{ei}). Collection 5 data were used in this study.

4. Results and Discussions

[17] Figure 1 is the global distribution of aerosol optical thickness (AOT) at 0.55 μm over both land and ocean for July 2005, excluding locations where the surface is too bright to retrieve the aerosol loading (e.g., the Sahara, Saudi Arabia, Greenland (M. D. King, personal communication, 2006)). Urban regions of North America, Europe, India, and East Asia have greater AOT than most of the inner continents, with the exception of biomass burning in Gabon and the Democratic Republic of the Congo, and dust outbreaks from the Sahara that are transported across the Atlantic. Over east China, AOT can be as high as 1.0, as a result of urban activities, aerosols transported from other regions, as well as biomass burning. However, it is useful to reiterate that *Zheng et al.* [2005] found that most of the aerosols in our study area are likely anthropogenic during July.

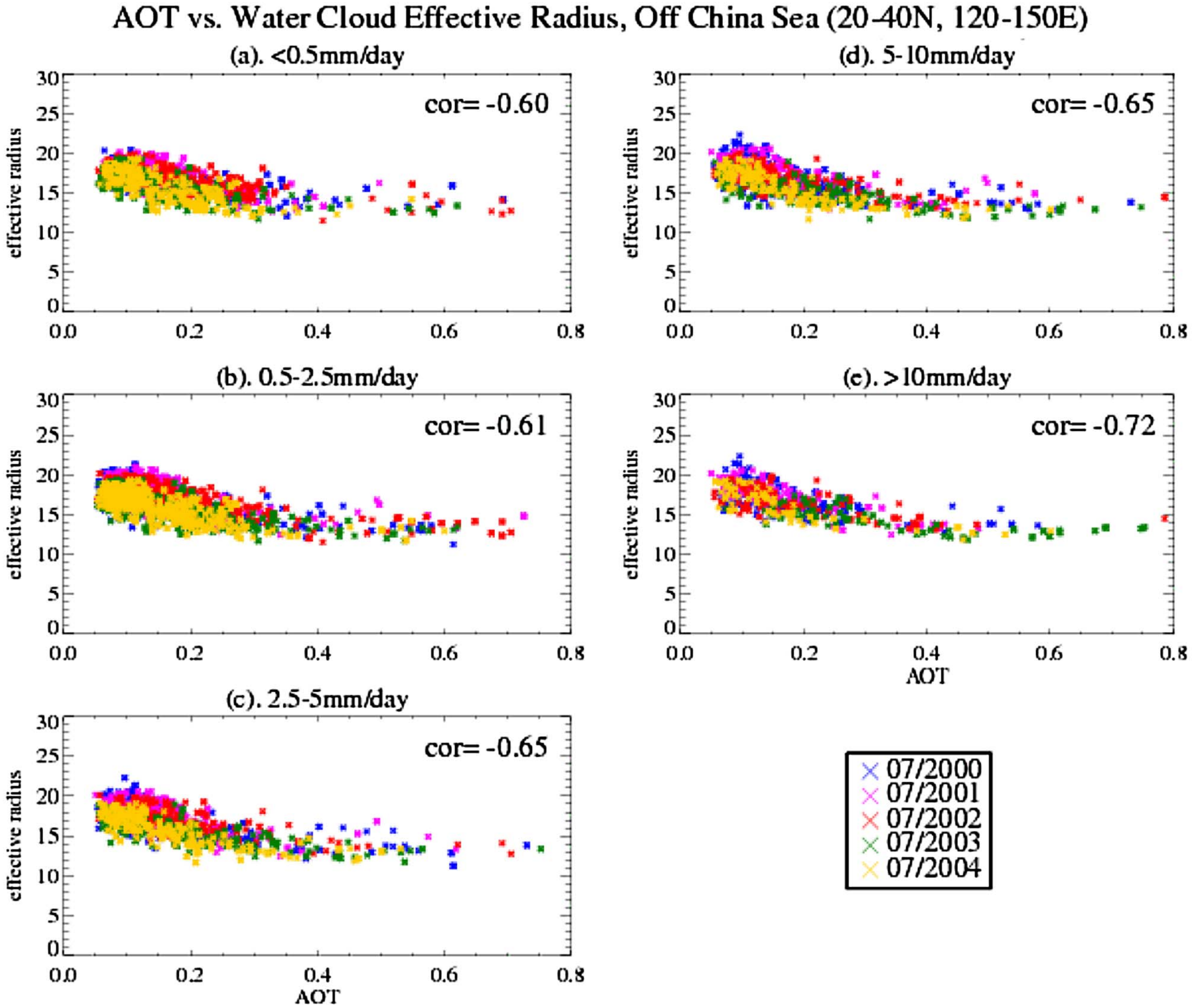

Figure 3. Scatterplot between aerosol optical thickness and water cloud effective radius. The data are sampled for Julys 2000–2004, over the China Sea (20°N–40°N, 120°E–150°E). Areas with monthly rainfall (a) less than 0.5 mm/d, (b) between 0.5 and 2.5 mm/d, (c) between 2.5 and 5.0 mm/d, (d) between 5 and 10 mm/d, and (e) larger than 10 mm/d.

[18] AOT over east China (110°E–120°E, 25°N–35°N) and in the China Sea (120°E–130°E, 25°N–35°N) has seasonal variability with the minimum occurring during winter and the maximum occurring from spring (April, May) to early summer (Figure 2). For example, over land, from April 2000 to April 2006, the maximum monthly mean AOT over urban regions occurred in June 2003, with a value of 0.84. The minimum monthly mean of AOT occurred in November 2000, with a value of 0.33. Such seasonality is partially due to the annual cycle of the biosphere, namely, large biomass burning in spring, and partially due to atmospheric chemical processes. During summer, photochemical interactions are more active owing to higher air temperatures, which increase certain aerosol concentrations in the atmosphere [*Dickerson et al.*, 1997]. Furthermore, AOT over ocean has similar seasonality to that of land, but its absolute values are always lower than land. This fact suggests that aerosols over the China Sea are primarily transported from urban regions.

4.1. Aerosol Versus Clouds

[19] Aerosol effects on clouds are examined through AOT and water cloud effective radius (r_{ew}) and ice cloud effective radius (r_{ei}), following previous studies of *Myhre et al.* [2006] and *Kaufman et al.* [2005], which revealed a negative relationship between aerosol optical thickness and cloud effective radius. Nevertheless, our results present how urban clouds droplet size and AOT relate, and how values could be useful for urban modeling in order to accurately represent urban AOT and r_{ei} [*Jin and Shepherd*, 2005]. Negative relationships between AOT and effective radius of water clouds are evident for all rainfall categories (Figure 3), namely, < 0.5 mm/d, 0.5–2.5 mm/d, 2.5–5.0 mm/d, 5–10 mm/d, and > 10 mm/d. The correlation coefficients

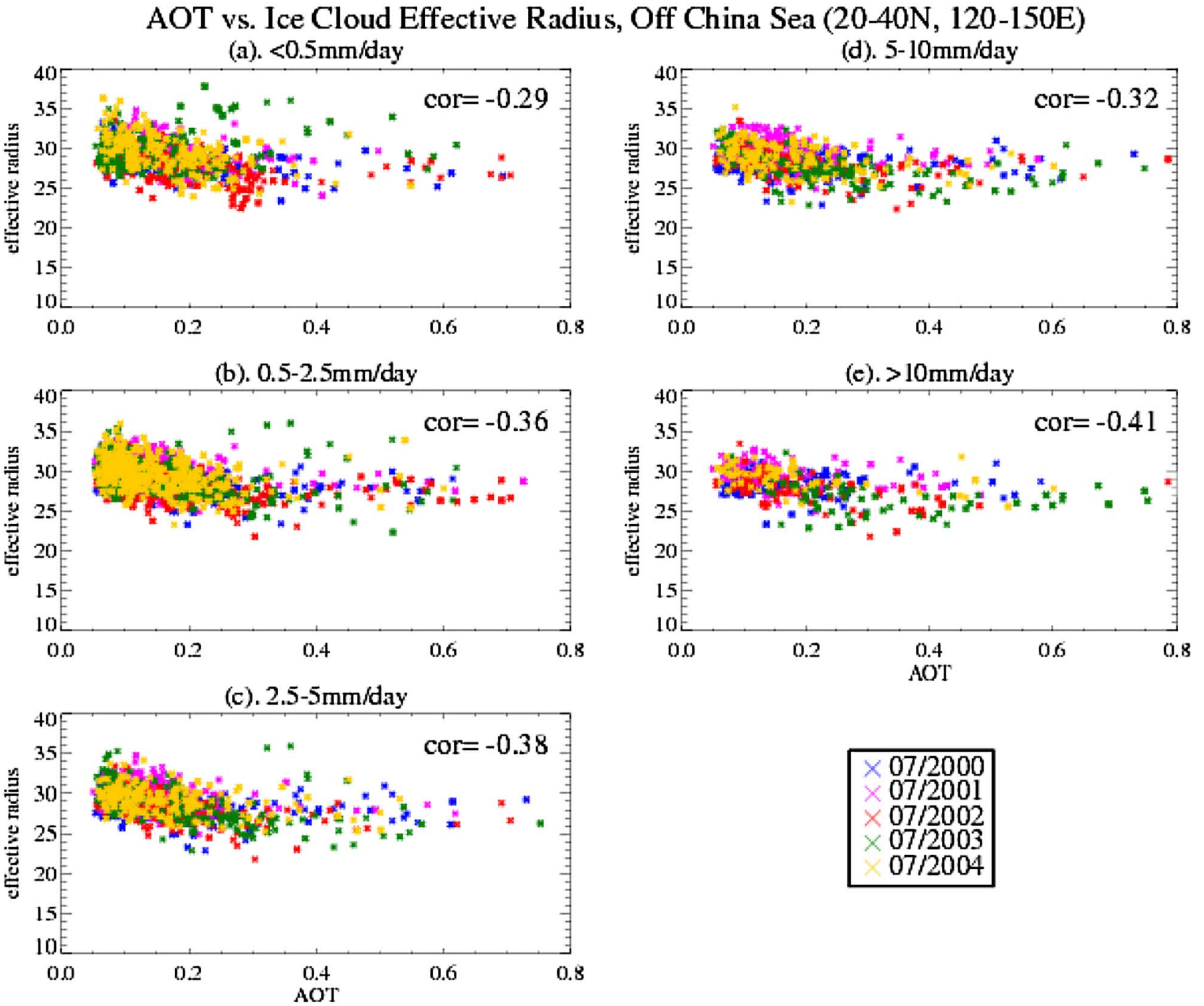

Figure 4. Scatterplot between aerosol optical thickness and ice cloud effective radius. The data are sampled for July 2000, over the China Sea.

between AOT and r_{ew} are negative, from −0.60 to −0.72, for all of the rainfall categories (Figure 3). When AOT is less than 0.2, the maximum r_{ew} can be up to 22 μm and when AOT increases to 0.6, the r_{ew} is about 15 μm. The negative relation between AOT and r_{ew} and means that more aerosols led to smaller water cloud effective radius, as predicted by *Twomey et al.* [1984]. Figure 3 is for all Julys (2000–2004). MODIS monthly mean water cloud fields are sampled for all water cloud pixels seen directly by the satellite during that month, and therefore the water cloud pixels used in Figure 3 represent warm clouds from which rainfall events occur. The strong negative relation between AOT and r_{ew} reflects a strong, negative relationship between aerosols and warm clouds. This is strong evidence for a negative relationship between AOD and r_{ew} and is consistent with previous literature.

[20] For ice clouds, on the other hand, aerosol effects are less significant than for water clouds (Figure 4). Since MODIS can only see the top of clouds, ice clouds correspond to cold and often high clouds. Figure 4 reveals that, in our study, aerosol effects are less significant on cold, high clouds than they are for warm clouds (namely, Figure 3). The correlation coefficients between AOT and r_{ei} are still negative but much lower than those for water clouds, namely, from −0.06 to −0.45, suggesting a weaker negative relation between AOT and r_{ei}.

[21] Over land, water cloud effective radius does not change as dramatically with AOT (Figure 5) for all Julys during 2000–2004. For all rainfall categories, the continental urban water clouds have r_{ew} around 15 μm. Similarly, ice cloud effective radius is also insensitive to change of aerosol optical thickness (Figure 6). Since aerosol presence over these regions is clearly detected (see Figure 1), aerosol effects on clouds are expected to reduce cloud droplet size. However, the unchanged r_{ew} observed here may suggests that although aerosols affect clouds, other competing mechanisms also affect clouds and eventually compensate for the aerosol effect. Studies have shown or hypothesized [e.g., *Shepherd*, 2005; *Changnon et al.*, 1976] that dynamics

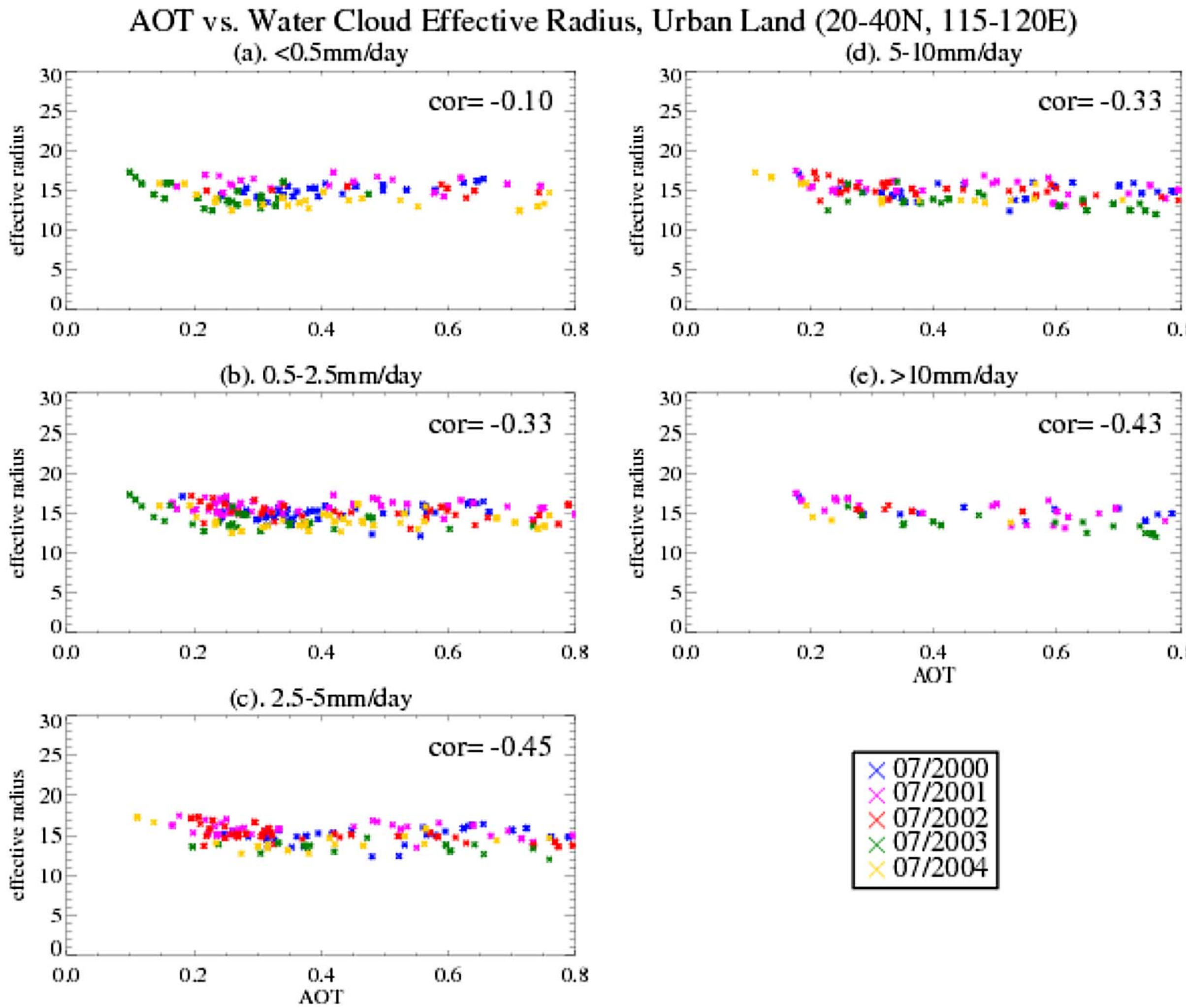

Figure 5. Scatterplot between aerosol optical thickness and water cloud effective radius. The data are sampled for Julys 2000–2004, east China urban regions (20°N–40°N, 115°E–120°E).

related to urban heat island-induced circulations and low-level convergence can initiate or enhance convective precipitation processes.

4.2. Aerosols Versus Rainfall

[22] Determined by large-scale dynamics, in particular the seasonal variation of the subtropical high, rainfall over the China Sea shows seasonality, namely, a relative maximum in the summer and a relative minimum in winter (Figure 7). Here, only convective rainfall rate is presented instead of total rainfall or stratiform rainfall, because convective rainfall, the dominant rainfall type during this season [*Ding*, 1994; *Wang et al.*, 2004], is more sensitive to the presence of aerosols in atmosphere. Nevertheless, although they show a semiopposite phase, the annual cycles of AOT and rainfall (Figure 7) likely do not show the linkage between these two components in the climate system. One explanation for this finding is that individual physical, chemical, or large-scale dynamic processes mainly determine their variability. The following analyses on AOT and rainfall are to examine if there is strong relationship between these two fields.

[23] When rainfall rate is less than 0.5 mm/d (Figure 8a), in a statistical sense, rainfall efficiency decreases with increasing aerosol optical thickness. The linear regression equation (Figure 8a, red line) is $G = 5.05 - 2.08AOT$. The negative slope, although small, establishes a sign of the negative relationship between AOT and G. The median-based regression equation (Figure 8a, green line) is $G = 15.11 - 12.61AOT$. One median is calculated from each of 10 optical thickness data entries. This resample rebuilds a new median subset from the original data set, and the median regression equation (shown in the green line in Figure 8a) is calculated on the basis of it. The median is statistically robust [*Wilks*, 1995], and thus the median regression equation (Figure 8a, green line) may be more statistically meaningful than the regression based on the original data (Figure 8a, red line). The relatively enhanced negative slope (-12.61) in the green line suggests that in larger aerosol cases, rainfall efficiency decreases. Note that similar negative relationships between AOT and G are also observed for June and August (not shown), suggesting that this may be a general case for summers. On the contrary, in January, such negative relationships are not detectable from

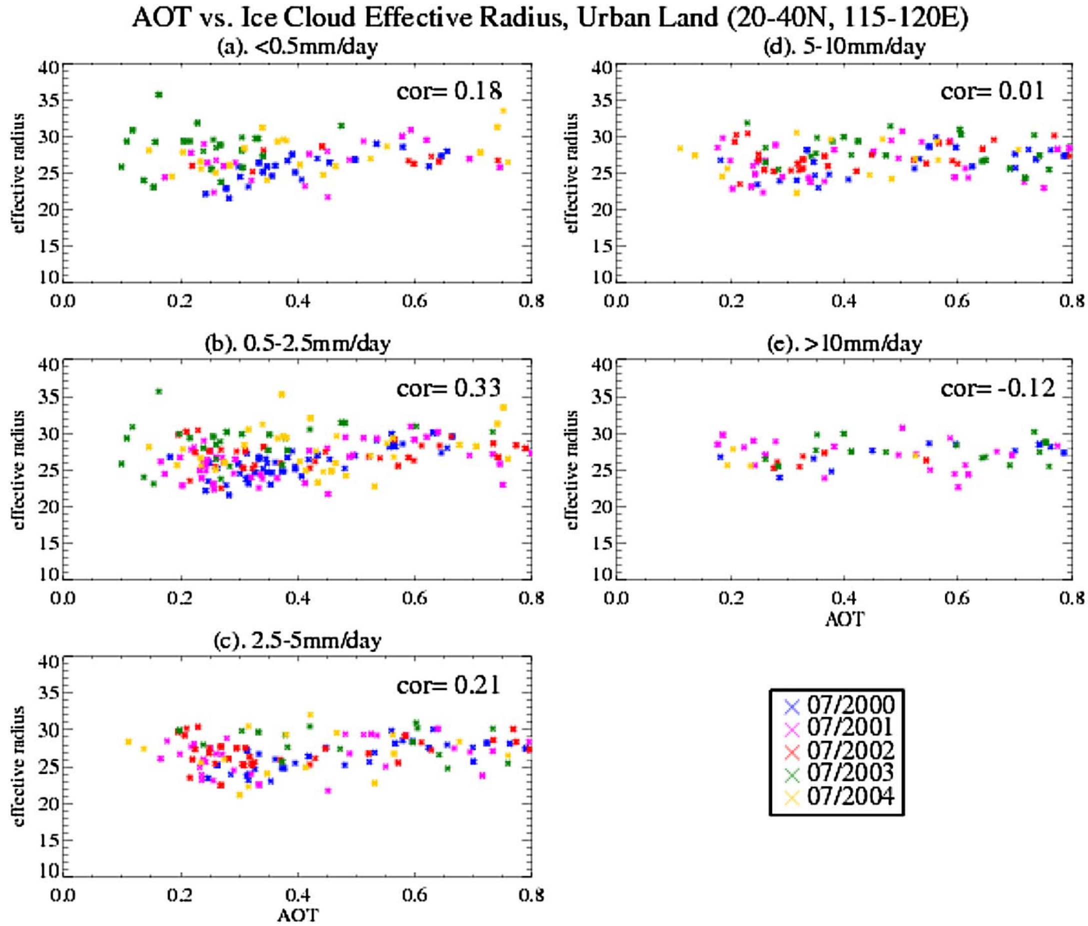

Figure 6. Scatterplot between aerosol optical thickness and ice cloud effective radius. The data are sampled for Julys 2000–2004, China urban regions (20–40°N, 115–120°E).

data we analyzed. The correlation coefficient between monthly AOT and G is −0.10 while the coefficient between median AOT and median Γ is −0.42.

[24] In addition, most of the light rainfall events occur when AOT is 0.1 (Figure 8b) since the peak of probability density function (PDF) is at AOT = 0.1. For higher AOT, fewer rainfall events occur. Careful interpretation is need here because it is possible that, in these regions and months where MODIS observes high AOT, the air may be reasonably cloud-free with corresponding low rain rates. However, it is also possible that the MODIS mask could be generating an association of low rain rates and high AOT. Another possibility is that areas with substantial rain tend to have low AOT just because of increased scavenging by the rain. We are aware of the uncertainty of interpreting this slightly negative slope, and keep seeking better approaches to examine these processes.

[25] Similar to light rainfall less than 0.5 mm/d, Figure 9 shows G and AOT for other rainfall categories. For rainfall averages between 0.5 mm/d and 2.5 mm/d (Figure 9b), the

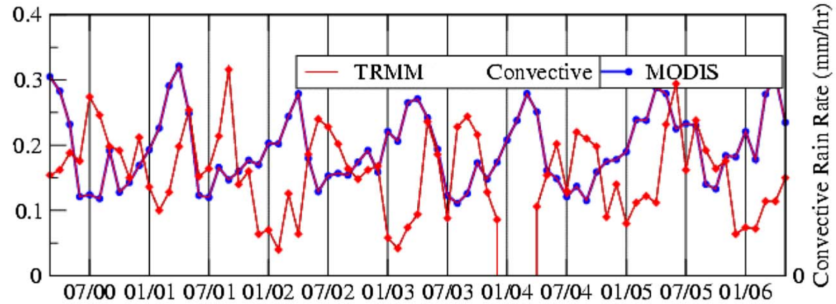

Figure 7. Interannual variations of urban aerosol (MODIS AOD) and TRMM convective rainfall rate (mm/h).

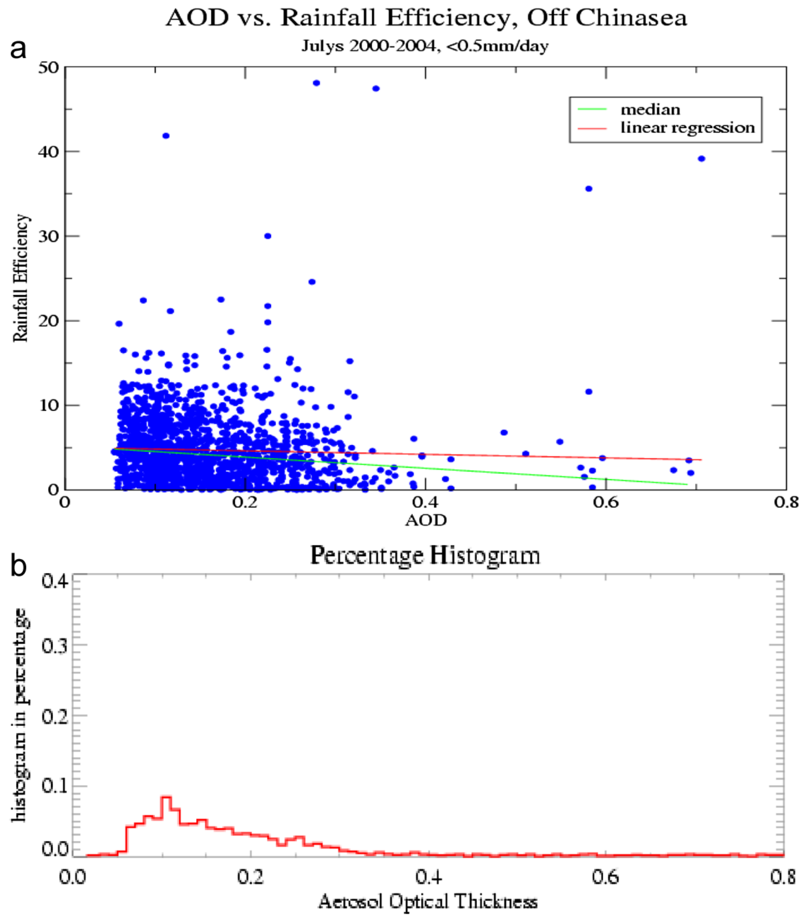

Figure 8. (a) Scatterplot of aerosol optical thickness and rainfall efficiency for rainfall events less than 0.5 mm/d, over the China Sea. The data are sampled for July (2000–2004). The red line is a linear regression based on original 5 July observations (blue dots); and the green line is the linear regression based on median. Median is calculated for each 10 optical thickness data. (b) Histogram of number of pixels as function of aerosol optical thickness.

median-based regression equation is G = 21.6–2.19 AOT. The small negative slope corresponds to the decrease of G with more aerosols. On the contrary, no negative regression equation or negative aerosol-rainfall relationship can be detected for relatively larger rainfall events, namely, 2.5–5.0 mm/d (Figure 9c), 5.0–10 mm/d (Figure 4d), and > 10 mm/d events. Nevertheless, it seems that the maximum G decreases at larger AOT, for all rainfall categories (Figures 9a–9e). Because large samples are needed in order to make such examination of slope meaningful, a few years of data are examined together instead of year to year. We also examined other summer regions along the south and east Asia coast and those results (not shown) also suggest a negative slope between AOT and light rainfall.

5. Final Remarks

[26] Results from this study, albeit more limited in record length and temporal scale than the optimal case, suggest that urban aerosols may have stronger effects on clouds than on rainfall. Using monthly mean aerosol optical thickness, effective radius of water and ice clouds, and rainfall efficiency, we found a detectable negative aerosol-cloud relationship, especially over the ocean. By contrast, a negative aerosol-rainfall signal is detectable only for light rainfall (rainfall rate < 2.5 mm/d) over ocean. These results suggest that aerosol effects are stronger for warm clouds, and weaker for rainfall, at least at the monthly scale. Although further work is required to verify this finding at other scales, our current results presented here may suggest that aerosols have more apparent effects on clouds than on rainfall. It supports current understanding that cloud formation is closely related to the aerosol presence while rainfall can be formed or augmented through many other dynamic processes.

[27] Aerosols may have different effects over ocean and over land. Over ocean, aerosols show significant effects on effective radius of liquid water clouds. There is less evidence for effects on ice clouds. On the other hand, over land (namely, continental areas with a large fraction of urban surfaces), no significant aerosol effects can be detectable in either water clouds or ice clouds. This finding further supports the hypothesis that over land, dynamics (e.g., destabilization, convergence) may play the dominant role in determining urban-modified clouds and rainfall [*Shepherd*, 2005]. Convection is strong over urban surfaces, owing to

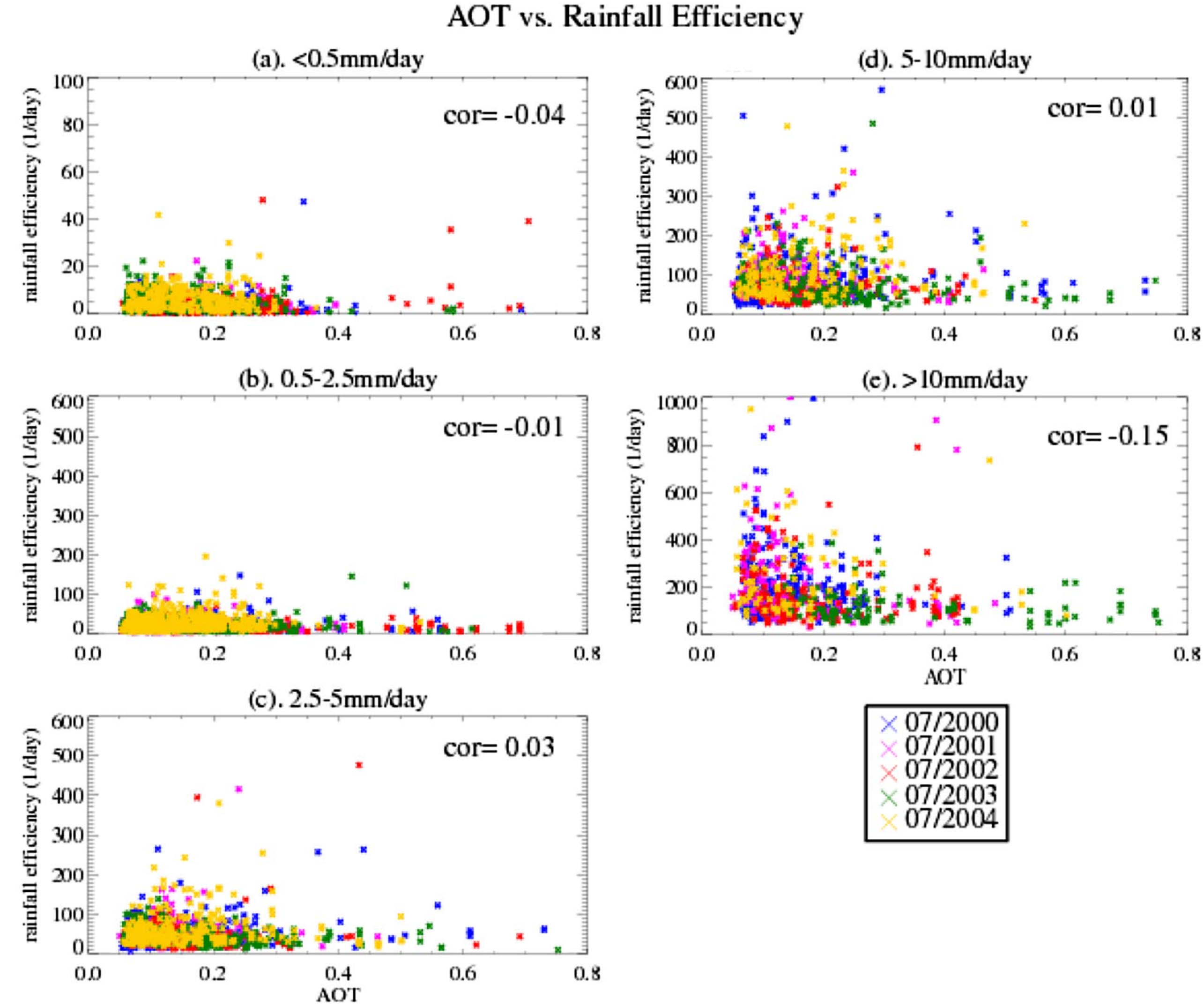

Figure 9. Scatterplot for rainfall and aerosol optical thickness. (a) Same as Figure 8a, (b) same as Figure 9a except for rainfall pixels 0.5–2.5 mm/d, (c) for rainfall pixels 2.5–5.0 mm/d, (d) for rainfall pixels 5–10 mm/d, and (e) for rainfall events larger than 10 mm/d. Data are from TRMM in the China Sea.

the enhanced surface heat island dynamics [*Jin et al.*, 2005b] and a more vigorous urban-induced land-atmosphere fluxes [*Shepherd and Burian*, 2003; *van den Heever and Cotton*, 2007]. The strong surface temperature gradient and related mesoscale circulations result in stronger convection that also affects cloud droplet formation. Convection has a competing effect on cloud effective radius formation, and thus reduces the aerosol signal for clouds. Over ocean, surface-induced convection is less significant owing to the lack of an urban thermal-dynamic gradient on the sea surface temperature. Therefore, the aerosol effect is more detectable on oceanic light rainfall events.

[28] Using various satellite platforms to conduct research will, as always, raise concerns about the correspondence among the measurements. The TRMM satellite does not view the China Sea equally at all hours of the day during a single month. The times of day missed by TRMM vary with the month. Meanwhile, MODIS only provides data at roughly noon and midnight. Naturally, a concern is that if rainfall varies with the time of day, the variations in TRMM viewing times could generate variations in monthly rainfall that appear unconnected with what MODIS observes. Such concern is part of the uncertainty of any research using satellites. Nevertheless, so far there is no solid evidence to show such uncertainty causes large error in rainfall and aerosol sampling. We should use the currently best available observations (here TRMM, SSMI, MODIS) to examine our previous understanding of aerosol-cloud-rainfall relationships and to consider the data limits when we interpret our results.

[29] It is beyond the scope of this paper to discuss the chemical properties of aerosols, but they have some effect on rainfall. For example, large particles are expected to form giant cloud condensation nuclei, which would produce larger cloud droplets that speed the formation of rain. However, dust particles are found to contain very little water-absorbing matter and thus even large dust particles form relatively small cloud droplets [*Rosenfeld*, 2000; *Yin et*

al., 2002]. These processes might be partly responsible for our observation of insignificant aerosol effects on rainfall.

[30] **Acknowledgments.** This work is supported by NASA TRMM Program Office and NASA PMM funding NNX07AF39G, as well as This research has been supported by the Defense Threat Reduction Agency. Special thanks go to Robert F. Adler and Ramesh Kakar, who provided finical supporting and extremely valuable suggestions on TRMM observations. Michael D. King provided insightful discussions on MODIS cloud data and interpretation.

References

Adler, R. F., G. J. Huffman, D. T. Bolvin, S. Curtis, and E. J. Nelkin (2000), Tropical rainfall distributions determined using TRMM combined with other satellite and rain gauge information, *J. Appl. Meteorol.*, *39*(12), 2007–2023, doi:10.1175/1520-0450(2001)040<2007:TRDDUT>2.0.CO;2.

Alishouse, J. C., J. B. Snider, E. R. Westwater, C. T. Swift, C. S. Ruf, S. A. Snyder, J. Vongsathorn, and R. R. Ferraro (1990), Determination of cloud liquid water content using the SSM/I, *IEEE Trans. Geosci. Remote Sens.*, *28*(5), 817–822.

Alpert, P., P. Kishcha, Y. J. Kaufman, and R. Schwarzbard (2005), Global dimming or local dimming? Effect of urbanization on sunlight availability, *Geophys. Res. Lett.*, *32*, L17802, doi:10.1029/2005GL023320.

Bell, T. L., D. Rosenfeld, K.-M. Kim, J.-M. Yoo, M.-I. Lee, and M. Hahnenberger (2008), Midweek increase in U.S. summer rain and storm heights suggests air pollution invigorates rainstorms, *J. Geophys. Res.*, *113*, D02209, doi:10.1029/2007JD008623.

Berg, W., T. L'Ecuyer, and C. Kummerow (2006), Rainfall climate regimes: The relationship of regional TRMM rainfall biases to the environment, *J. Appl. Meteorol. Climatol.*, *45*, 434–445.

Burian, S. J., and J. M. Shepherd (2005), Effects of urbanization on the diurnal rainfall pattern in Houston: Hydrological processes, *Hydrol. Processes*, *19*, 1089–1103, doi:10.1002/hyp.5647.

Carrico, C. M., M. H. Bergin, J. Xu, K. Baumann, and H. Maring (2003), Urban aerosol radiative properties: Measurements during the 1999 Atlanta Supersite Experiment, *J. Geophys. Res.*, *108*(D7), 8422, doi:10.1029/2001JD001222.

Changnon, S. A., Jr., R. G. Semonin, and F. A. Huff (1976), A hypothesis for urban rainfall anomalies, *J. Appl. Meteorol.*, *15*(6), 544–560.

Dickerson, R. R., S. Kondragunta, G. Stenchikov, K. L. Civerolo, B. G. Doddridge, and B. N. Holben (1997), The impact of aerosols on solar ultraviolet radiation and photochemical smog, *Science*, *278*, 827–830, doi:10.1126/science.278.5339.827.

Ding, Y. (1994), *Monsoon Over China*, 419 pp., Kluwer Acad., Dordrecht, Netherlands.

Duncan, B. N., R. V. Martin, A. C. Staudt, R. Yevich, and J. A. Logan (2003), Interannual and seasonal variability of biomass burning emissions constrained by satellite observations, *J. Geophys. Res.*, *108*(D2), 4100, doi:10.1029/2002JD002378.

Iguchi, T., T. Kozu, R. Meneghini, J. Awaka, and K. Okamoto (2000), Rain-profiling algorithm for the TRMM precipitation radar, *J. Appl. Meteorol.*, *39*(12), 2038–2052, doi:10.1175/1520-0450(2001)040<2038:RPAFTT>2.0.CO;2.

Jacobson, M. Z., and Y. J. Kaufman (2006), Wind reduction by aerosol particles, *Geophys. Res. Lett.*, *33*, L24814, doi:10.1029/2006GL027838.

Jin, M., and J. M. Shepherd (2005), On including urban landscape in land surface model—How can satellite data help?, *Bull. Am. Meteorol. Soc.*, *86*(5), 681–689.

Jin, M., J. M. Shepherd, and M. D. King (2005a), Urban aerosols and their interaction with clouds and rainfall: A case study for New York and Houston, *J. Geophys. Res.*, *110*, D10S20, doi:10.1029/2004JD005081.

Jin, M., R. E. Dickinson, and D.-L. Zhang (2005b), The footprint of urban areas on global climate as characterized by MODIS, *J. Clim.*, *18*(10), 1551–1565, doi:10.1175/JCLI3334.1.

Joseph, J. H., Y. J. Kaufman, and Y. Mekler (1991), Urban light pollution—The effect of atmospheric aerosol on astronomical observations at night, *Appl. Opt.*, *30*, 3047–3058.

Jung, T., E. Ruprecht, and F. Wagner (1998), Determination of cloud liquid water path over the oceans from Special Sensor Microwave/Imager (SSM/I) data using neural networks, *J. Appl. Meteorol.*, *37*(8), 832–844, doi:10.1175/1520-0450(1998)037<0832:DOCLWP>2.0.CO;2.

Kaufman, Y. J., D. Tanre, and O. Boucher (2002), A satellite view of aerosols in the climate system, *Nature*, *419*, 215–223, doi:10.1038/nature01091.

Kaufman, Y. J., I. Koren, L. A. Remer, D. Rosenfeld, and Y. Rudich (2005), The effect of smoke, dust, and pollution aerosol on shallow cloud development over the Atlantic Ocean, *Proc. Natl. Acad. Sci. U.S.A.*, *102*(32), 11,207–11,212, doi:10.1073/pnas.0505191102.

King, M. D., W. P. Menzel, Y. J. Kaufman, D. Tanre, B.-C. Gao, S. Platnick, S. A. Ackerman, L. A. Remer, R. Pincus, and P. A. Hubanks (2003), Cloud and aerosol properties, precipitable water, and profiles of temperature and humidity from MODIS, *IEEE Trans. Geosci. Remote Sens.*, *41*(2), 442–458, doi:10.1109/TGRS.2002.808226.

King, M. D., S. Platnick, P. Yang, G. T. Arnold, M. A. Gray, J. Riedi, S. A. Ackerman, and K. N. Liou (2004), Remote sensing of liquid water and ice cloud optical thickness and effective radius in the Arctic: Application of airborne multispectral MAS data, *J. Atmos. Oceanic Technol.*, *21*, 857–875, doi:10.1175/1520-0426(2004)021<0857:RSOLWA>2.0.CO;2.

Lau, K. M., and K. M. Kim (2006), Observational relationships between aerosol and Asian monsoon rainfall, and circulation, *Geophys. Res. Lett.*, *33*, L21810, doi:10.1029/2006GL027546.

Lau, K. M., M. K. Kim, and K. M. Kim (2006), Asian monsoon anomalies induced by aerosol direct effect, *Clim. Dyn.*, *26*, 855–864, doi:10.1007/s00382-006-0114-z.

Lensky, I. M., and R. Drori (2007), A satellite-based parameter to monitor the aerosol impact on convective clouds, *J. Appl. Meteorol. Climatol.*, *46*, 660–666, doi:10.1175/JAM2487.1.

Li, C., L. T. Marufu, R. R. Dickerson, Z. Li, T. Wen, Y. Wang, P. Wang, H. Chen, and J. W. Stehr (2007), In situ measurements of trace gases and aerosol optical properties at a rural site in northern China during East Asian Study of Tropospheric Aerosols: An International Regional Experiment 2005, *J. Geophys. Res.*, *112*, D22S04, doi:10.1029/2006JD007592.

Li, Z., and T. Yuan (2006), Exploring aerosol-cloud-climate interaction mechanisms using the new generation of earth observation system data, in *Current Problems in Atmospheric Radiation*, edited by H. Fischer and B.-J. Song, pp. 1–4, A.A. Deepak, Hampton, Va.

Mote, T. L., M. C. Lacke, and J. M. Shepherd (2007), Radar signatures of the urban effect on precipitation distribution: A case study for Atlanta, Georgia, *Geophys. Res. Lett.*, *34*, L20710, doi:10.1029/2007GL031903.

Myhre, G., F. Stordal, M. Johnsrud, Y. J. Kaufman, D. Rosenfeld, T. Storelvmo, J. E. Kristjansson, T. K. Berntsen, A. Myhre, and I. S. A. Isaksen (2006), Aerosol-cloud interaction inferred from MODIS satellite data and global aerosol model, *Atmos. Chem. Phys. Discuss.*, *6*, 9351–9388.

Nakajima, T., and M. D. King (1990), Determination of the optical thickness and effective particle radius of clouds from reflected solar radiation measurement. Part 1: Theory, *J. Atmos. Sci.*, *47*, 1878–1893, doi:10.1175/1520-0469(1990)047<1878:DOTOTA>2.0.CO;2.

National Research Council (2006), *Assessment of Benefits of Extending the Tropical Rainfall Measuring Mission*, Natl. Acad. Press, Washington, D.C.

Platnick, S., M. D. King, S. A. Ackerman, W. P. Menzel, B. A. Baum, J. C. Riédi, and R. A. Frey (2003), The MODIS cloud products: Algorithms and examples from Terra, *IEEE Trans. Geosci. Remote Sens.*, *41*(2), 459–473, doi:10.1109/TGRS.2002.808301.

Post, J. E., and P. R. Buseck (1984), Characterization of individual particles in the Phoenix urban aerosol using electron-beam instruments, *Environ. Sci. Technol.*, *18*, 35–42, doi:10.1021/es00119a009.

Ramanathan, V., P. J. Crutzen, J. T. Kiehl, and D. Rosenfeld (2001), Aerosols, climate, and the hydrological cycle, *Science*, *294*, 2119–2124, doi:10.1126/science.1064034.

Remer, L. A., and Y. J. Kaufman (1998), Dynamic aerosol model: Urban/industrial aerosol, *J. Geophys. Res.*, *103*, 13,859–13,872, doi:10.1029/98JD00994.

Rosenfeld, D. (2000), Suppression of rain and snow by urban and industrial air pollution, *Science*, *287*, 1793–1796, doi:10.1126/science.287.5459.1793.

Rosenfeld, D., J. Dai, X. Yu, Z. Yao, X. Xu, X. Yang, and C. Du (2007), Inverse relations between amounts of air pollution and orographic precipitation, *Science*, *315*, 1396–1398, doi:10.1126/science.1137949.

Shepherd, J. M. (2005), A review of current investigations of urban-induced rainfall and recommendations for the future, *Earth Interact.*, *9*, 1–27, doi:10.1175/EI156.1.

Shepherd, J. M., and S. J. Burian (2003), Detection of urban-induced rainfall anomalies in a major coastal city, *Earth Interact.*, *7*, 1–14, doi:10.1175/1087-3562(2003)007<0001:DOUIRA>2.0.CO;2.

Shepherd, J. M., H. Pierce, and A. J. Negri (2002), On rainfall modification by major urban areas: Observations from space-borne radar on TRMM, *J. Appl. Meteorol.*, *41*, 689–701, doi:10.1175/1520-0450(2002)041<0689:RMBMUA>2.0.CO;2.

Simpson, J., R. F. Adler, and G. R. North (1988), A proposed tropical rainfall measuring mission (TRMM) satellite, *Bull. Am. Meteorol. Soc.*, *69*, 278–295, doi:10.1175/1520-0477(1988)069<0278:APTRMM>2.0.CO;2.

Trenberth, K. E. et al. (2007), Observations: Surface and atmospheric climate change, in *Climate Change 2007: The Physical Science Basis*.

Contribution of Working Group I to the Fourth Assessment Report of the Intergovernmental Panel on Climate Change, edited by S. Solomon et al., pp. 235–336, Cambridge Univ. Press, Cambridge, U. K.
Twomey, S. A., M. Piepgrass, and T. L. Wolfe (1984), An assessment of the impact of pollution on global cloud albedo, *Tellus, Ser. B*, *36*, 356–366.
Vallina, S., R. Simo, and S. Gasso (2006), What controls CCN seasonality in the Southern Ocean?: A statistical analysis based on satellite-derived chlorophyll and CCN model-estimated OH radical and rainfall, *Global Biogeochem. Cycles*, *20*, GB1014, doi:10.1029/2005GB002597.
van den Heever, S. C., and W. R. Cotton (2007), Urban aerosol impacts on down wind convective storms, *J. Appl. Meteorol. Climatol.*, *46*, 828–850, doi:10.1175/JAM2492.1.
Wang, B., L. Ho, Y. Zhang, and M.-M. Lu (2004), Definition of South China Sea Monsoon onset and commencement of the East Asia Summer Monsoon, *J. Clim.*, *17*(44), 669–710.
Wentz, F. J., and R. W. Spencer (1998), SSM/I rain retrievals within a unified all-weather ocean algorithm, *J. Atmos. Sci.*, *55*, 1613–1627, doi:10.1175/1520-0469(1998)055<1613:SIRRWA>2.0.CO;2.
Wilks, D. S. (1995), *Statistical Methods in the Atmospheric Sciences*, 464 pp., Academic Press, San Diego, Calif.
Yin, Y., S. Wurzler, Z. Levin, and T. G. Reisin (2002), Interactions of mineral dust particles and clouds: Effects on precipitation and cloud properties, *J. Geophys. Res.*, *107*(D23), 4724, doi:10.1029/2001JD001544.
Zhao, C., X. Tie, and Y. Li (2006), A possible positive feedback of reduction of precipitation and increase in aerosols over eastern central China, *Geophys. Res. Lett.*, *33*, L11814, doi:10.1029/2006GL025959.
Zhao, F., and Z. Li (2007), Estimation of aerosol single scattering albedo from solar direct spectral radiance and total broadband irradiances measured in China, *J. Geophys. Res.*, *112*, D22S03, doi:10.1029/2006JD007384.
Zheng, M., L. Salmon, J. Schauer, L. Zeng, C. Kiang, Y. Zhang, and G. Cass (2005), Seasonal trends in PM2.5 source contributions in Beijing, China, *Atmos. Environ.*, *39*, 3967–3976, doi:10.1016/j.atmosenv.2005.03.036.

M. Jin, Department of Meteorology, San José State University, San José, CA 95192-0104, USA. (jin@met.sjsu.edu)

J. M. Shepherd, Atmospheric Sciences Program, Department of Geography, University of Georgia, Athens, GA 30602, USA. (marshgeo@uga.edu)